JOURNAL OF GEOPHYSICAL RESEARCH, VOL. 105, NO. A12, PAGES 27,611–27,620, DECEMBER 1, 2000

Electron acceleration by Alfvén waves in density cavities

V. Génot[1] and P. Louarn

Centre d'Etude Spatiale des Rayonnements, Toulouse, France

F. Mottez

Centre d'Etude des Environnements Terrestre et Planétaires, Vélizy, France

Abstract. A new electromagnetic two-dimensional guiding center particle in cell (PIC) code is used to investigate the propagation of an Alfvén wave in the perpendicular density gradients that characterize the edges of the auroral density cavities. It is shown that the wave planes are strongly distorted by the inhomogeneities of the plasma and that a significant electric field develops in the direction parallel to the background magnetic field during the propagation. This field efficiently accelerates the electrons in the parallel direction, and the incident wave is thus strongly absorbed. The associated dissipation rate is sufficiently strong to explain a complete wave absorption on the density gradients over a fraction of wavelength. The electron parallel acceleration is also characterized. It corresponds to a global parallel acceleration of the electron population. These PIC simulations suggest that the perpendicular density gradients corresponding to the auroral plasma cavities play an important role in the auroral particle acceleration.

1. Introduction

The auroral particle acceleration is a still not understood mechanism of general astrophysical interest. It is indeed related to the existence of electric fields in the direction parallel to the static magnetic field. However, the extremely large parallel conductivity of the collisionless plasmas is expected to immediately short-circuit them. The formation of fields able to explain the energization of particles up to the 10-keV energy range, over spatial and temporal scales compatible with the observations (a few thousand kilometers along the magnetic field, for seconds to minutes timescales), then remains an open issue.

Over the years, many theoretical ideas have been developed. Some of them are related to microscopic processes that may (1) introduce a finite conductivity in the auroral circuit system (anomalous resistivity concept; see the review of *Papadopoulos* [1977]), (2) create a potential difference by the accumulation of small-scale nonlinear structures (the weak double-layer model [*Block,* 1972; *Temerin et al.,* 1982; *Mozer et al.,* 1983; *Boström et al.,* 1988; *Mälkki et al.,* 1993; *Koskinen et al.,* 1990; *Mottez et al.,* 1992] in the auroral region context and [*Mangeney et al.,* 1999] in the solar wind context), or (3) directly transfer energy from high-frequency waves to the particle populations (interaction with lower hybrid waves [*Bingham et al.,* 1984]). At a radically different scale, other models describe the possible existence of a global ionosphere/magnetosphere electrostatic potential difference over the whole auroral field lines (the strong double-layer model (see, for example, *Miura and Sato* [1980]) and the kinetic model initially proposed by *Alfvén and Fälthammar* [1963] (see also *Chiu and Schulz* [1978])). Although these models are useful for getting a large-scale and static view of the auroral regions, a different line of thought deliberately favors the inherent dynamical nature of the auroral phenomena. Thus in the kinetic/inertial Alfvén wave model [*Hasegawa,* 1976], the parallel electric field results from electron inertia effects that modify the dispersion of shear Alfvén waves in very oblique propagation (typically, $k_\perp c/\omega_{pe} \sim 1$).

The Alfvén wave model was recently the subject of a growing interest, since observations by the Freja, Fast and Interball spacecraft [*Louarn et al.,* 1994; *Wahlund et al.,* 1994; *Seyler et al.,* 1995; *Volwerk et al.,* 1996; *Stasiewicz et al.,* 1998; *Knudsen,* 1996; *Chust et al.,* 1998; *Chaston et al.,* 1999] have definitively proven the important role of the low-frequency electromagnetic fluctuations in the auroral energization processes [*Gurnett et al.,* 1984; *Boehm et al.,* 1990; *Berthelier et al.,* 1991; *Gustafsson et al.,* 1990]. On the theoretical side, this model has been developed in many different ways. For example, *Goertz and Boswell* [1979] have shown that Alfvén wave packets can present some of the prop-

[1]Now at Astronomy Unit, Queen Mary, University of London, London, England, United Kingdom.

Paper number 1999JA000341.
0148-0227/00/1999JA000341$09.00

erties of electrostatic shocks. In the framework of a linear model (no effect of the accelerated electrons on the wave packet is taken into account), the resulting direct electron energization and the consecutive modifications of the velocity distribution functions have been studied by *Kletzing* [1994]. In a series of papers [*Lysak and Dum,* 1983; *Lysak,* 1990; *Lysak and Lotko,* 1996], dynamic models of the ionosphere/magnetosphere coupling that links the anomalous resistivity concept and the Alfvén wave propagation were proposed. They can be related to models describing the linear Alfvén wave propagation over the complete field line in relation with the formation of auroral structures [*Streltsov and Lotko,* 1995, 1999] in the sense that both types of studies propose a global view of the auroral processes based on particular features of the Alfvén waves propagation. Various aspects of the nonlinear Alfvén waves propagation have also been studied in order to describe the formation of small perpendicular scales in the wave packet and the creation of parallel electric fields (see, for example, *Chmyrev et al.* [1989], *Bellan and Stasiewicz* [1998], *Shukla et al.* [1999], *Seyler* [1990], and *Seyler and Wahlund* [1996]). Recently, one-dimensional self-consistent simulations have been used to describe the nonlinear evolution of large-amplitude inertial Alfvén waves and the formations of electron beams [*Clark and Seyler,* 1999].

Despite their variety, these models have all neglected a possible important aspect of the auroral regions: their strong density organization in directions perpendicular to the magnetic field. Small length scale cavities have indeed been observed in the auroral zone by Viking, Freja, and more recently by the Fast spacecraft, at altitudes ranging from 2000 km to 12,000 km. They correspond to density reduction by factors of 5 to 10 over a few kilometers. They are rather systematically related to the presence of a strong electrostatic turbulence and the formation of upgoing and downgoing electron beams. More generally, these density cavities thus appear to be the favorite sites of the particle acceleration and, following Viking and Fast results, related to the generation of auroral kilometric radiation [*Louarn et al.,* 1990; *Hilgers,* 1992; *Hilgers et al.,* 1992; *Carlson et al.,* 1998; *Strangeway et al.,* 1998; *Ergun et al.,* 1998]. In order to understand their potential importance for the acceleration, we recently proposed a model based on modifications of the Alfvén wave characteristics due to the propagation in the density cavity [*Génot et al.,* 1999] (hereinafter referred to as paper 1). Using a simplified linear model in the cold plasma approximation, we have shown that the propagation of an Alfvén wave on the density gradients that characterize the edges of the cavities leads (1) to the rapid formation of small length scales of the order of c/ω_{pe} and (2) to the development of large-scale parallel electric fields able to accelerate particles up to the observed energies. However, this first study suffers from a lack of self-consistency and does not include the calculation of the energy dissipation.

In the present paper, we extend this first study and we describe the self-consistent wave/particle evolution that takes place during the propagation in the plasma cavities. Using a new gyrokinetic two-dimensional (2-D) electromagnetic particle in cell (PIC) code that takes into account the complete ion dynamics and uses an electron guiding center approximation (the code is described in section 2), we simulate the Alfvén wave propagation in a plasma cavity, and we study the formation of the parallel electric field (section 3). The energy transfer from the wave to the different particle populations is estimated (section 4), and we give evidence for the particle acceleration consecutive to the formation of parallel electric fields on the density gradients. The associated deformations of the distribution functions are discussed in section 5, before the conclusions (section 6).

2. Description of Simulation Method

The acceleration processes at work in auroral regions are intrinsically at least bidimensional. They involve simultaneously large magnetohydrodynamic (MHD) scales (Alfvén waves in parallel propagation) and small-scale kinetic effects (interaction with the gradients, inertial effects). For physical reasons, neither the MHD codes nor the hybrid codes that do not include any kinetic effect on the electron can address the above mentioned issues. On the other hand, the classical kinetic explicit codes (explicit PIC or Vlasov codes) are too demanding, in terms of computational time and memory, to allow 2-D simulations over temporal and spatial scales of interest for the present study. For these reasons, we have developed a new implicit 2.5-D (2-D space, 3-D field and velocity components) electromagnetic gyrokinetic code well adapted to the study of the propagation of Alfvén waves. This code has been extensively described by *Mottez et al.* [1998].

It is basically an electromagnetic PIC code. The plasma is then considered as an assembly of macroparticles, whose motions are computed individually. They depend on the electromagnetic field interpolated at the position of each particle from a grid. The electromagnetic field is then computed on the grid by using the Maxwell equations and the charge and current densities deduced from the positions and velocities of the macroparticles. The motion of the ions (or macroions) is computed from the Lorentz force. The originality of the code lies in the description of the electron dynamics. Indeed, as in the strongly magnetized auroral plasma, the mean electron Larmor radius is small in comparison with all other characteristic lengths, and the electron dynamics are well modeled by their guiding centers. The code thus simulates the motion of the electron guiding centers, taking into account all the guiding

center drifts. This is described [*Northrop,* 1963] by the equation

$$\dot{\mathbf{v}} = -\frac{e}{m}[\mathbf{E}(\mathbf{r}) + \mathbf{v} \times \mathbf{B}(\mathbf{r})] - \frac{\mu}{m}\nabla B(\mathbf{r}). \quad (1)$$

When simulating an electromagnetic plasma with an explicit PIC code [*Birsdall and Langdon,* 1985; *Hockney and Eastwood,* 1988], several timescales must be taken into account. The aim of an implicit code is to solve the evolution equations of a dynamical system without keeping the high-frequency fluctuations. In the direct implicit scheme, a few variables of the system (at time step n) are replaced by time-averaged implicit variables. These implicit variables depend on the state of the system both in the past (time $n-1$) and in the future (time $n+1$) [*Langdon et al.,* 1983; *Hewett and Langdon,* 1987]. The implicit scheme is then solved by using a predictor-corrector algorithm.

A rough classification of timescales in a plasma can help us to understand which physical parameters must be made implicit, according to the problem to be treated. The higher frequencies are generally those of the light waves which propagate at velocity c. Light waves do not interfere with the plasma, but the stability conditions of an explicit electromagnetic field equation solver requires that these waves be described. We use an electromagnetic field equation solver that is implicit over the light waves.

The following range of frequencies (after the light wave high frequencies), in our case where $\omega_{ce} \geq \omega_{pe}$, is associated with the high-frequency oscillations caused by the electron gyromotion. When the magnetic gradients are not too high, as in our case where the mean electron Larmor radius is small in comparison with all relevant characteristic lengths, the guiding center approximation gives a good description of the electron motion in a magnetized plasma and allows the use of a time step that is large in comparison with an electron gyroperiod. Our code uses an integration scheme that allows the description of the ion full dynamics and the electron guiding center dynamics, based on the direct implicit algorithm, accurate to the second order in Δt.

Here are displayed the equations that contain implicit terms. The other equations, like those of the ion motion and of the charge and the current density, are the same as those in explicit PIC codes [*Birsdall and Langdon,* 1985; *Hockney and Eastwood,* 1988]. The finite differenced Maxwell's equations are

$$\mathbf{E}_{n+1} - \mathbf{E}_n = c^2\Delta t\nabla \times \mathbf{B}_{n+1/2} - \frac{1}{\epsilon_0}\Delta t\mathbf{J}_{n+1/2}. \quad (2)$$

The electric current includes the electron guiding center magnetization current $-\nabla \times \mu\mathbf{b}$ that comes from the variation of the magnetic field seen by the electrons during their gyromotion around their guiding center.

$$\mathbf{B}_{n+1/2} - \mathbf{B}_{n-1/2} = -\Delta t\nabla \times \bar{\mathbf{E}}_n \quad (3)$$

$$\mathbf{B}_{n+1} - \mathbf{B}_{n+1/2} = -\frac{1}{2}\Delta t\nabla \times \mathbf{E}_{n+1} \quad (4)$$

$$\bar{\mathbf{E}}_n = \frac{1}{2}[\mathbf{E}_{n+1} + \bar{\mathbf{E}}_{n-1}]. \quad (5)$$

The implicit guiding center equations of motion are

$$\mathbf{v}_{n+1/2} = \mathbf{v}_{n-1/2} + \Delta t[-\frac{e}{m}\mathbf{E}_n - \frac{\mu}{m}\nabla B_n(\mathbf{x}_n) - \frac{e}{2m}(\mathbf{v}_{n+1/2} + \bar{\mathbf{v}}_{n-1/2}) \times \mathbf{B}_n(\mathbf{x}_n)] \quad (6)$$

$$\mathbf{x}_{n+1} = \mathbf{x}_n + \Delta t\mathbf{v}_{n+1/2} \quad (7)$$

$$\bar{\mathbf{v}}_{n+1/2} = \frac{1}{2}[\mathbf{v}_{n+1/2} + \bar{\mathbf{v}}_{n-3/2}]. \quad (8)$$

The magnetic moment μ, which is the first adiabatic invariant, is supposed to be constant. Moreover, a correction for the parallel velocity is taken into account. For more details and explanations about these equations and the way they are solved, see *Mottez et al.* [1998].

As electron inertial effects may be important in the interaction of an Alfvén wave with a density gradient (creation of an inertial Alfvén wave), we have kept the description of the plasma oscillations. Therefore our code can resolve timescales of the order of ω_{pe}^{-1} and has a spatial resolution of one Debye length λ_D. In the auroral case (at least at high altitudes where $\omega_{ce} \geq \omega_{pe}$), such a code saves an important fraction of the computational time in comparison with a classical PIC code. This is a crucial point for realistic 2-D simulations of the Alfvén wave propagation. By construction, the code is completely self consistent and retains nonlinear phenomena.

The ion to electron mass ratio is reduced to 100. The typical simulation box is a grid of 2048×32 cells having an individual size of $0.01(c/\omega_{pe})^2$. The box thus physically corresponds to ~1000 km in the parallel direction and ~20 km in the transverse direction, assuming a density of 1 cm^{-3}. Since the length of a grid cell must be of the order of or smaller than a Debye length λ_D, this choice also fixes a lower limit value for the electron temperature (thermal velocity of $0.1c$, in the present case). A total number of 4×10^6 particles are taken into account. The running time covers several Alfvén periods.

To model the cavity, we use a channel-like configuration (Figure 1) with density gradients presenting a typical scale of c/ω_{pe} (larger than the ion Larmor radius). It is important to note that as far as the finite ion Larmor radius effect is neglected (which here corresponds to the fact that the density gradient scale is large in comparison with the ion gyroradius), the channel is in MHD equilibrium. It indeed corresponds to the polarization of a perpendicular slow magnetosonic wave, whose frequency is equal to zero. Moreover, for this particular polarization angle, this slow magnetosonic solution includes the nonlinearities. The polarization is given by $B = B_z$ and $c_s^2\Delta\rho(x) = -(1/2\mu_0)\Delta B_z^2$, where c_s is the

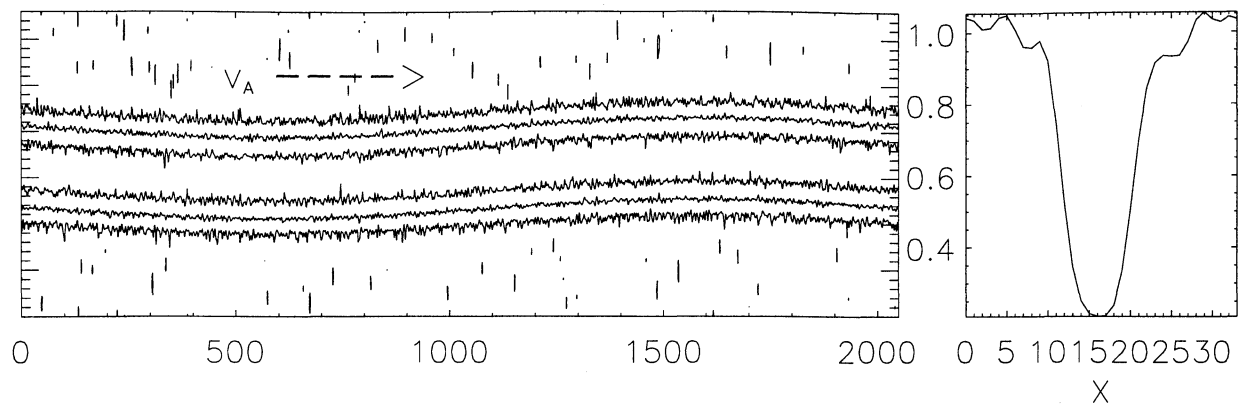

Figure 1. Electron density profile after a few time steps of the simulation. (left) Contours; (right) cut along x for $z = 10$.

sound velocity, $\Delta\rho(x)$ is the variation of the density, and ΔB_z^2 is the change (along x) of the square root of the magnetic field. As the frequency and the polarization are independent of the wavelength, any density profile $\rho(x)$ is possible. We have set a uniform temperature all over the simulation domain. The simulation domain initially contains three zones of constant density and two zones with a constant gradient. The stability of the initial configuration has been checked directly by the simulations. In the absence of incoming Alfvén waves and for the range of density gradients studied in the following, no particular phenomena are observed, and the channel-like configuration stays at rest.

The ambient magnetic field is parallel to the z axis. Its amplitude is such that $\omega_{ce}/\omega_{pe} = 4$. Our choice of the other simulation parameters is a compromise between the computer limits and the respect of the ordering of the auroral plasma parameters. We have chosen $\lambda_D(= 0.1c/\omega_{pe}) < \rho_L(= 0.25c/\omega_{pe}) \leq c/\omega_{pe}$, where ρ_L is the ion Larmor radius. In comparison, at Viking altitudes, this ordering is typically $\lambda_D(= 0.02c/\omega_{pe}) < \rho_L(= 0.2c/\omega_{pe}) \leq c/\omega_{pe}$. This difference ($\lambda_D < \rho_L$ in the simulation and $\lambda_D \ll \rho_L$ in reality) is mainly a consequence of the reduced mass ratio. It can be important for some particular physical mechanisms. However, in the present case and concerning the Alfvén wave propagation, the different scales modify the dispersion relation and control the formation of a nonvanishing parallel electric field through the terms $k_\perp c/\omega_{pe}$, $k_\perp \rho_L$, or $k_\perp \lambda_D$, where $k_\perp$ is the perpendicular wave number. In a situation of sudden incoming of Alfvén waves in the cavity, it is important to respect the first scale at which the dissipation may occur. This scale is c/ω_{pe} for both the simulation and the auroral plasma. For this reason, we expect that the simulation retains the most important phenomena linked to the Alfvén wave dissipation in the auroral regions.

For this first study, we have used a system periodic in both the x and z directions (y is the direction of invariance). Clearly, simulations of nonperiodic systems, especially in the direction of the magnetic field (z, here), would be of the highest interest in the context of the auroral physics. With such nonperiodic codes, it would be possible, for example, to follow the propagation of a wave packet from the magnetospheric side and to study its progressive absorption and the associated particle acceleration as it enters the regions on density inhomogeneity. This kind of simulation nevertheless constitutes a very difficult task for the type of codes used here, and its development is planned for the future. Nevertheless, one has to note that in the particular context of auroral physics, periodic codes along the magnetic field direction can provide interesting results. Let us comment on this point.

To obtain a linear polarization of the incoming wave, we initialize the system with the superposition of an Alfvén wave and a fast magnetosonic wave propagating along the ambient magnetic field ($k = k_z = k_\parallel$). The characteristics of the initial waves (phase velocity, for example) are adapted to the plasma conditions existing outside the density channel. At $t = 0$, we thus impose to the system a time-varying electromagnetic field corresponding to waves that are not expected to be adapted to the channel configuration. This is an analysis of the impulsive response of the plasma that actually corresponds to the auroral situation. In case of a sudden increase of the electromagnetic energy flux from the magnetosphere into the structured auroral plasma, the Alfvén velocity in the auroral region is indeed so large (10^5 km/s at an altitude of 10^4 km) that a low-frequency electromagnetic wave enters the auroral cavities in a short time (0.1 s for a cavity of 10^4-km height) compared with its typical period (1 s). The analysis of the impulsive response of a static inhomogeneous plasma to the sudden arrival of an electromagnetic flux has then a lot in common with the actual situation.

The amplitude of the waves is given by the ratio $\delta B/B_0$ of the perturbed magnetic field over the ambient magnetic field. We use high $\delta B/B_0$ ratios (0.01 to 0.05) to overcome the inherent thermal noise of the

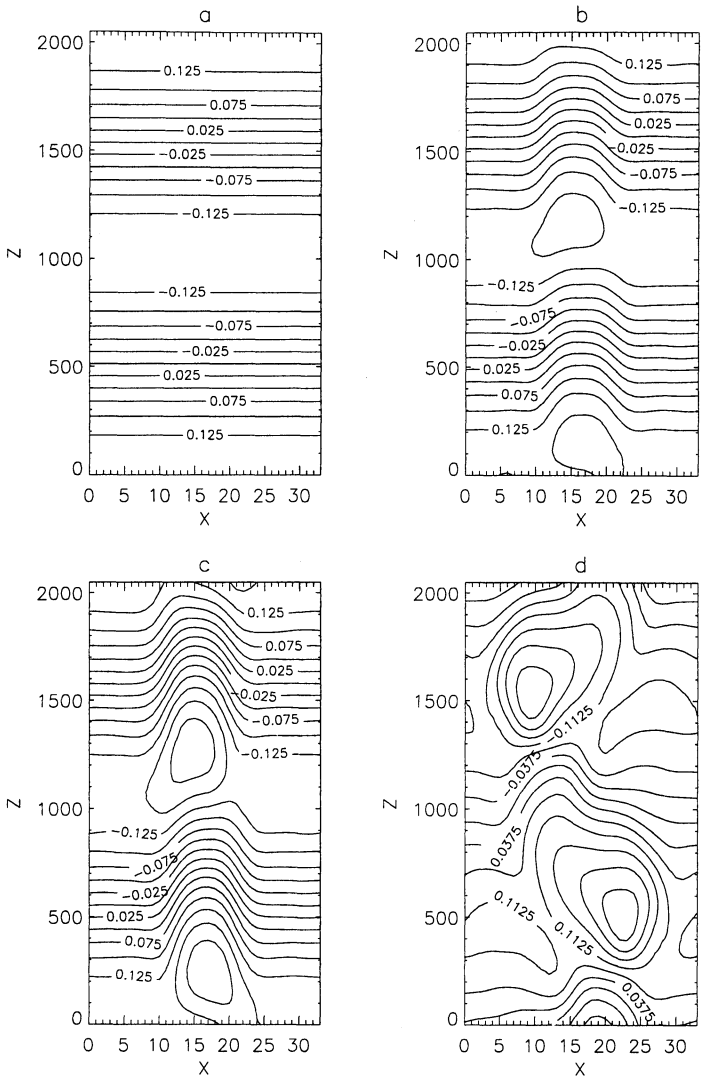

Figure 2. Normalized perpendicular component ($eE_x/\omega_{pe}cm_e$) of the electric field at times 0 (a), 8 ω_{pe}^{-1} (b), 16 ω_{pe}^{-1} (c), and 128 ω_{pe}^{-1} (d). The wave period is 512 ω_{pe}^{-1}.

simulation. The phase velocity is $0.326c$ ($0.815v_A$) for the Alfvén wave and $0.415c$ ($1.038v_A$) for the fast magnetosonic wave.

3. Development of Small Perpendicular Scales and Generation of Parallel Electric Field

The first noticeable effect of the density gradients on the Alfvén wave propagation is the fast distortion of the wave front. Since the Alfvén velocity is larger in the center of the channel region than on the sides, small length scale structures in the wave front are quickly created, and the initial purely parallel wave vector $\vec{k}$ turns in to exhibit a significant $k_\perp$. This is a way to explain the progressive rotation of the wave vector during the propagation; the perpendicular component is here not taken a priori as is often the case in inertial Alfvén wave (IAW) studies (like that of *Kletzing* [1994]). This is shown in Figures 2a-c. The initially strictly parallel level contours of E_x become curved on the locus of the density gradient. In the present case, perpendicular scales of the order of c/ω_{pe} in the wave front appear in a small fraction (1/20 typically) of the wave period. This effect is important in the context of IAW propagation, since it contributes to the formation of parallel electric field. In the simple linear study proposed in paper 1 this evolution was not limited, and arbitrary small perpendicular scales were obtained for sufficiently long parallel propagation. This is not observed in the present, more complex simulation. In Figures 2a-c, we only present the first stages of the evolution. Later (see Figure 2d), even if the electric field has a more complex structure, its typical perpendicular scale does not significantly evolve toward smaller scales. On a linear basis, there is no reason to stop the scale evolution at c/ω_{pe},

the critical scale at which new effects appear being the ion Larmor radius ($0.2c/\omega_{pe}$). In the present discussion, this subsequent nonevolution can be interpreted as an effect of the dissipation and of the interaction with the density gradient.

From a simplified linear model (no density variations along the ambient magnetic field $\vec{B}_0$), one obtains (see paper 1)

$$\frac{\partial E_\parallel}{\partial z} = -\frac{c^2}{v_A^2 \omega_{pe}^2} \frac{\partial^2}{\partial t^2} \left(\frac{\partial E_x}{\partial x} + \frac{\partial \ln n}{\partial x} E_x \right) \qquad (9)$$

where z (x) is the direction parallel (perpendicular) to $\vec{B}_0$.

Two terms can thus be responsible for the formation of $E_\parallel$. In the range of auroral parameters ($\beta \ll 1$), the first term of the right-hand side is of the form $k_\parallel k_\perp c^2/\omega_{pe}^2 E_x$, where $k_\perp \sim 1/E_x \partial E_x/\partial x$ and $k_\parallel \sim 1/E_x \partial E_x/\partial z$. Thanks to this term, the distortion of the wave front contributes to the formation of $E_\parallel$ which corresponds to classical IAW. The parallel field (and thus the wave/electron energy exchange) is expected to increase as smaller perpendicular scales are reached. This would induce an enhanced wave dissipation at small scale and thus stop the linear wave front evolution toward smaller scales. In the presence of strong density gradients, the second term of the right-hand side can also be important and even dominant as soon as $1/n \partial n/\partial x \geq k_\perp$. The interpretation of this term is the following. During the Alfvén wave (AW) propagation, the polarization drift: $j_x = m_i n_i / B^2 \partial E_x/\partial t$, pushes the ions in the transverse direction on a large parallel extension. Such a displacement induces a space charge on the density gradient locus (see Figure 3a). Two effects are then expected. First, the space charge will induce the formation of a perpendicular field with a typical scale related to the scale of the density gradient (Poisson equation). This contributes to the nonevolution of the electric field perpendicular scale already mentioned. Second, in the low β auroral plasma, the nonneutrality can only be restored by the longitudinal dynamics of the particles, hence the formation of a parallel electric field. Let us illustrate these different effects.

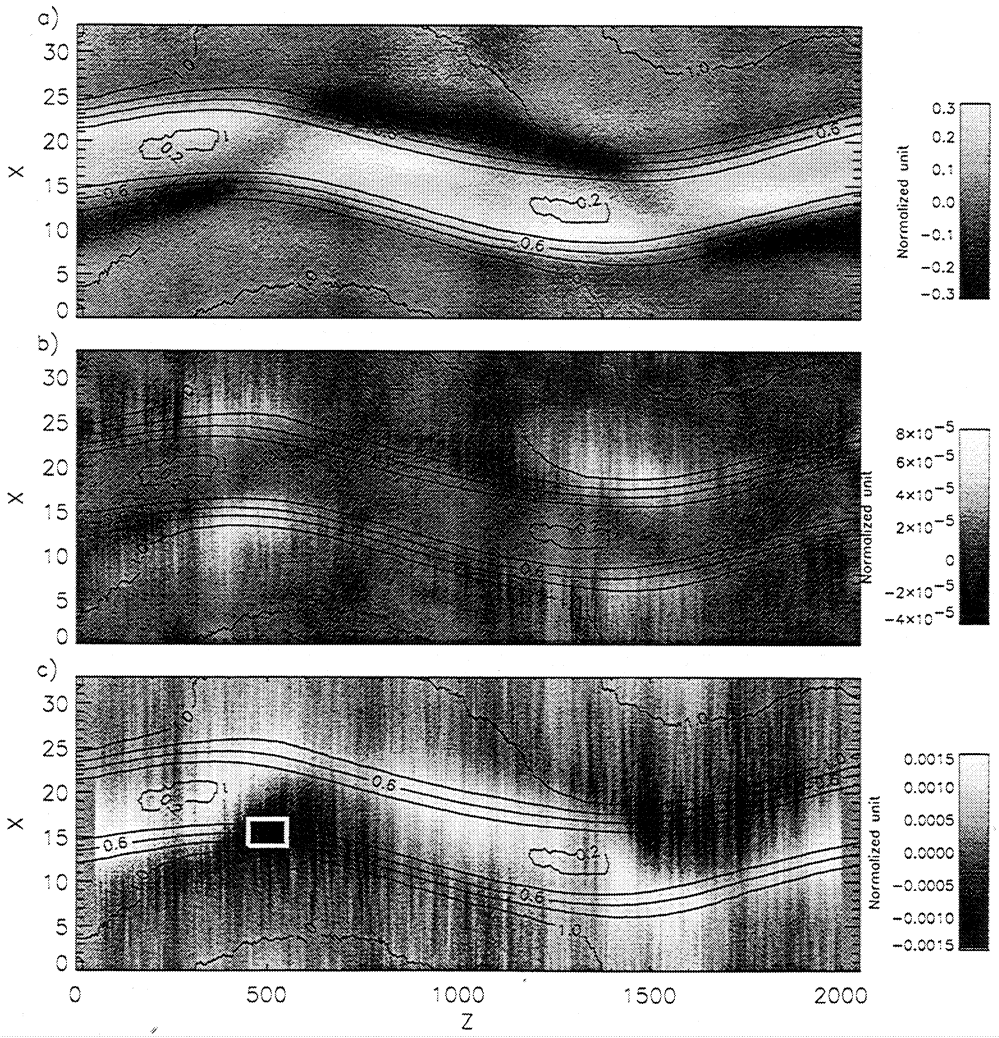

Figure 3. Space charge ($(n_i - n_e)/n_0$), dissipation rate ($j_\parallel \cdot E_\parallel / n_0 m_e c^2 \omega_{pe}$), and parallel electric field ($eE_\parallel/\omega_{pe} c m_e$) at time 200 ω_{pe}^{-1} ($\omega_{pe}^2 = n_0 e^2/\epsilon_0 m_e$).

As is shown in Figures 3a and 3c, nonvanishing values of both the space charge and the parallel electric field appear quickly during the simulation (less than half the wave period). The normalized amplitudes are given by a grey scale, and the contours of the electron densities are superimposed, in order to localize the density gradients. During the simulation, the ratio $E_\parallel/E_\perp$ remains almost constant (about 0.01). In the absence of a density gradient and for an equivalent $k_\perp$ ($k_\perp c/\omega_{pe} \simeq 1$), this ratio would be 0.005, that is, half as large. In fact, the value of the parallel electric field can be coarsely calculated by the same expression as that for the IAW [e.g., *Goertz*, 1986] but where $k_\perp$ is replaced by $1/n\partial n/\partial x$

$$\frac{E_\parallel}{E_\perp} = \frac{k_\parallel}{\frac{1}{n}\frac{\partial n}{\partial x}} \frac{\left(\frac{c}{n\omega_{pe}}\frac{\partial n}{\partial x}\right)^2}{1+\left(\frac{c}{n\omega_{pe}}\frac{\partial n}{\partial x}\right)^2}. \tag{10}$$

The peaks of $E_\parallel$ (negative around [x =15, z =500] and [x =20, z =1500] and positive around [x =25, z =500] and [x =8, z =1500]) are clearly located on the gradient locus, where the polarization drift induced by the perpendicular electric field leads to the largest space charge. Moreover, following equation (1), the sign of $E_\parallel$ is linked to the sign of the gradient (briefly, $E_\parallel \propto \frac{\partial n}{\partial x}E_\perp$). In the plot, one also notes that the density channel oscillates around its initial position owing to the $\vec{E}_y \times \vec{B}_0$ drift, independent of the particle charge. This is not an important effect, but it is amplified by our representation as the scales on both axes are very different: 2048 cells in z compared with 32 cells in x.

The process of formation of the parallel electric field observed here is quite different from the one linked to the pure IAW propagation which would require the progressive formation of large $k_\perp$. In the present case, a significant parallel electric field appears during the very initial stage of the simulation. It is due to the effect described above, and it is directly linked to the existence of the density gradient. Whatever the $k_\perp$ of the electromagnetic perturbation propagating on the gradient, a parallel electric field will appear and will act directly on the particles. This could have important consequences in the context of auroral acceleration, since this means that waves belonging to a much larger spectral domain in $k_\perp$ than in the classical Alfvén wave model of the acceleration can efficiently contribute to particle energization. More generally, one can consider that any kind of low-frequency electromagnetic fluctuation presenting an adapted polarization (the perpendicular electric field must have a nonnull component in the density gradient direction) can contribute to the acceleration as it propagates into the density cavity.

4. Action on the Particles

To put into relief the energy transfer from the wave to the electrons, we calculate the total electron kinetic energy integrated in a region moving at v_A and where $E_\parallel$ has a constant sign. The mobile calculation box warps during the propagation to follow the gradients where $E_\parallel$ forms. The energy integrated in this box is plotted as a function of time in Figure 4. The increase in energy is about 25% over one Alfvén wave period. It can be checked that this can be regarded as an increase in the parallel kinetic energy of the electrons as they move preferentially in that direction.

In this plot, we can notice an oscillation of period $\sim 250\omega_{pe}^{-1}$. The corresponding frequency is twice the Alfvén wave frequency. This oscillation confirms that the transfer of energy to the electrons is made through nonlinear interactions with the Alfvén wave. The factor 2 between the frequencies indicates that this interaction is dominated by quadratic effects (quadratic terms associated with a wave with a frequency which is twice the wave frequency).

As is shown in Figure 3b, where the dissipation rate $j_\parallel \cdot E_\parallel$ is calculated for the entire simulation box, the energy transfer mainly occurs on the density gradient. The extrema of the dissipation rate are obtained on the gradient where $E_\parallel$ maximizes. Moreover, one notes that the maxima are given for the negative values of $E_\parallel$. This suggests that the energy transfer is more efficient when the particles are accelerated in the direction of the wave propagation, i.e., when they are susceptible to exchange of more energy with the wave (equivalent to a resonant process). This fact holds even after one wave period and is likely to hold also in an auroral situation. However, after this time and on this particular point, the link between these simulations and auroral physics becomes less relevant (because of the periodicity), as was previously pointed out. Using the maximum dissipation rate, one estimates the typical length over which the Poynting flux $\mathcal{P}_\parallel$ may be absorbed:

$$\Delta z \simeq \frac{\Delta \mathcal{P}_\parallel}{|j_\parallel \cdot E_\parallel|}. \tag{11}$$

For the simulation presented in Figure 3, one obtains $\Delta z \simeq 64\ c/\omega_{pe}$, which represents the third of the parallel wavelength. This emphasizes the fact that on the density gradients, where the dissipation rate maximizes, the wave Poynting flux can be dissipated on less than a wavelength. This gives an indication of the efficiency of the wave/particle energy transfer that is expected to occur at the density gradients.

To specify the type of particle acceleration consecutive to this energy transfer, we computed the potential drop associated with $E_\parallel$. For instance, in the region $400 < z < 600$ in Figure 3c, where the field has a maximum, one obtains $e|\Phi|/mc^2 = 0.02$, which corresponds to 4 times the thermal energy. Such large parallel potential drops will undoubtedly affect the particles, and as far as the distribution functions are concerned, one may expect a strong deviation from the initial Gaussian shape. This is shown in Figure 5, where the velocity distribution function for the electrons contained in the box

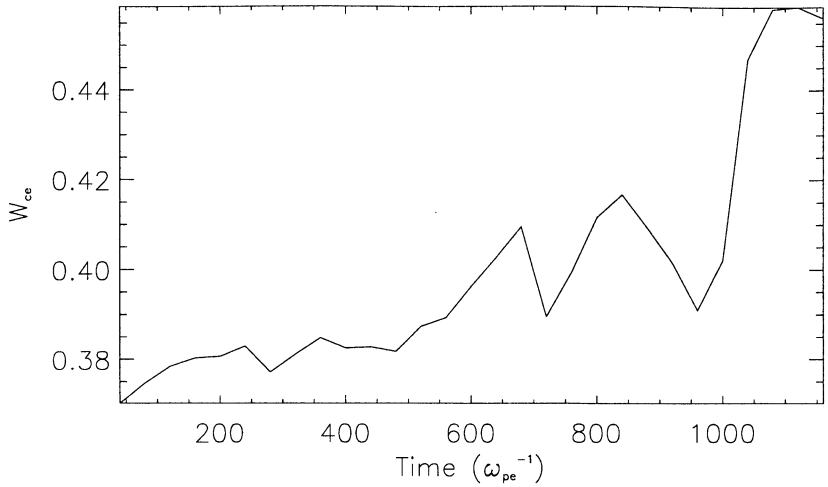

Figure 4. Electron kinetic energy integrated in a region of high values of the parallel electric field.

drawn in Figure 3c, where $|E_{||}|$ maximizes, is plotted. One notes a complete shift of the function (that now peaks at 0.05c) which denotes a global response of the electron bulk to the accelerating parallel electric fields. This type of distortion of the distribution functions suggests that these light particles immediately react to the parallel electric field applied. We do not detect a particular parallel heating or the formation of a beam in the present simulation.

Let us note that the energy transfer observed during the simulation results from a direct interaction between the electron population and the parallel electric field, and it is not equivalent to a classical dissipation of the wave electromagnetic energy due to a resonant effect. In the present simulation, which lasts only a few Alfvén wave periods, only the initial state of the wave/particle interaction is described. It corresponds to a progressive phasing between the particles (here the electrons in parallel motion) and the wave. Later, one may expect that an equilibrium state is reached in the simulation, with a periodic exchange of energy from the electromagnetic field to the particles. However, this equilibrium state is likely not reached for an Alfvén wave entering the auroral cavity. The electrons directly accelerated by the parallel electric field of the AW are indeed precipitated and lost in the ionosphere and cannot subsequently participate in the energy exchange. The energy exchange that actually occurs on the edges of a plasma cavity as the Alfvén wave propagates into it could thus present analogies with the particle acceleration observed at least during the initial period of the simulation (over one or two Alfvén wave periods).

The ion distribution function does not present any change, and no particular ion/wave energy exchange has been observed. In theory, an ion energization (heating) would have been observed if length scales down to the ion Larmor radius were created during the simulation. As was already discussed, this is not the case, mainly

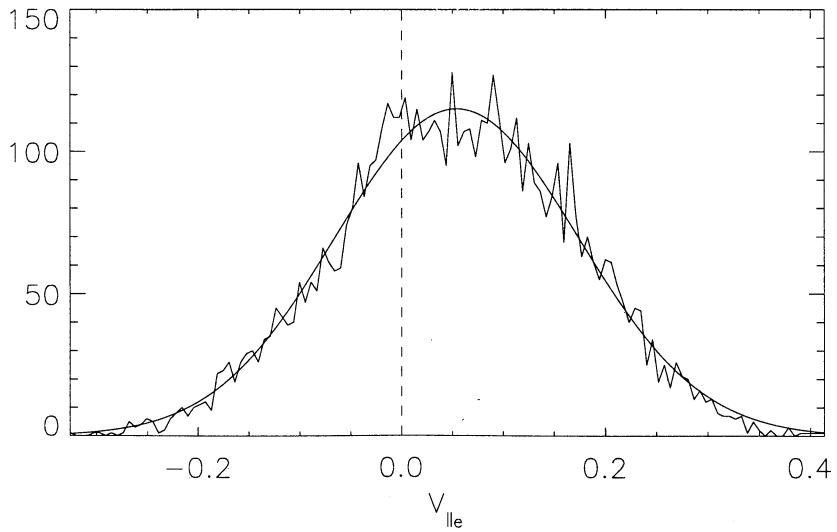

Figure 5. Velocity distribution function for the electrons where $|E_{||}|$ maximizes.

because during the linear cascade the first energy exchange (and then the wave dissipation) takes place at c/ω_{pe} and concerns the electron parallel acceleration.

5. Conclusion

In the present article, we have presented results of 2-D kinetic simulations of Alfvén waves propagating in a strongly inhomogeneous low-β plasma presenting analogies with the auroral plasma (the presence of density cavities). These simulations were done by using a new 2-D electromagnetic and gyrokinetic code. They mainly consist in the analysis of the impulsive response of the inhomogeneous plasma to a sudden variation of the electromagnetic energy flux and give some indications concerning the wave/particle interactions occurring in the small-scale auroral plasma cavities. The main conclusions are the following:

1. It is shown that the wave spectrum of an incoming Alfvén wave cascades to small length scales (c/ω_{pe}) in less than one wave period and that, simultaneously, large parallel electric fields arise on the density gradient locus. This leads to a significant wave/electron energy transfer. Nevertheless, in contrast to classical models of the electron acceleration by inertial Alfvén waves (in homogeneous plasma), the initial spectrum of the wave (in $k_\perp$) coming from the magnetosphere seems to have a rather minor importance in the formation of the parallel electric field. Indeed, for sufficiently short scale gradients, comparable to those actually observed in the auroral plasma, the spatial density variation is at the origin of the leading term in the apparition of the parallel electric field.

2. The linear wave cascade is limited typically to a scale of the order of c/ω_{pe}. This is the first scale at which dissipation occurs during the cascade. It corresponds to the parallel electron acceleration, and consequently, the ion heating that would occur at smaller scale is not observed for the range of parameters taken into consideration here.

3. The simulations show that the wave/particle interactions locally result in a global shift of the electron velocity distribution functions in the parallel direction. The typical energy gain corresponds to the mean potential drop obtained by an integration of the parallel electric field along the density gradients.

These three points, which will be studied in more detail in the future, suggest that a large fraction of the energy flux associated with the Alfvén wave propagation could be transferred into particle energy in the density cavities. This proves the possible importance of the perpendicular density gradients in the auroral acceleration processes.

Acknowledgments. The authors are grateful to D. Le Quéau for his helpful comments. The numerical computations have been supported by the CNRS and were made on the C98 at the IDRIS computation center (France).

Janet G. Luhmann thanks the referees for their assistance in evaluating this paper.

References

Alfvén, H., and C. G. Fälthammar, *Cosmical Electrodynamics*, pp. 163-167, Clarendon, Oxford, England, 1963.

Bellan, P. M., and K. Stasiewicz, Fine-scale cavitation of ionospheric plasma caused by inertial Alfvén wave ponderomotive force, *Phys. Rev. Lett., 80,* 3523, 1998.

Berthelier, A., J. C. Cerisier, J. J. Berthelier. and L. Rezeau, Low frequency magnetic turbulence in the high-latitude topside ionosphere: Low-frequency waves or field-aligned currents?, *J. Atmos. Terr. Phys., 53,* 333, 1991.

Bingham, R., D. A. Bryant, and D. S. Hall, A wave model for the aurora, *Geophys. Res. Lett., 11,* 327, 1984.

Birsdall, C. K., and B. Langdon, *Plasma Physics via Computer Simulation*, McGraw-Hill, New York, 1985.

Block, L. P., Potential double layers in the ionosphere, *Cosmic Electrodyn., 3,* 349, 1972.

Boehm, M. H., C. W. Carlson, J. P. McFadden, J. H. Clemmons, and F. S. Mozer, High-resolution sounding rocket observations of large-amplitude Alfvén waves, *J. Geophys. Res., 95,* 12,157, 1990.

Boström, R., G. Gustafsson, B. Holback, G. Holmgren, H. Koskinen, and P. Kintner, Characteristics of solitary waves and weak double layers in the magnetospheric plasma, *Phys. Rev. Lett., 61,* 82, 1988.

Carlson, C. W., et al., Fast observations in the downward auroral current region: Energetic upgoing electron beams, parallel potential drops, and ion heating, *Geophys. Res. Lett., 25,* 2017, 1998.

Chaston, C. C., C. W. Carlson, W. J. Peria, R. E. Ergun, and J. P. McFadden, Fast observations of inertial Alfvén waves in the dayside aurora, *Geophys. Res. Lett., 26,* 647, 1999.

Chiu, Y. T., and M. Schulz, Self-consistent particle and parallel electrostatic field distributions in the magnetospheric-ionospheric auroral region, *J. Geophys. Res., 83,* 629, 1978.

Chmyrev, V. M, et al., Non-linear Alfvén wave generator of auroral particles and ELF/VLF waves, *Planet. Space Sci., 37,* 749, 1989.

Chust, T., P. Louarn, M. Volwerk, H. de Feraudy, A. Roux, J. Wahlund, and B. Holback, Electric fields with a large parallel component observed by the Freja spacecraft: Artifacts or real signals?, *J. Geophys. Res., 103,* 215, 1998.

Clark, A. E., and C. E. Seyler, Electron beam formation by small-scale oblique inertial Alfvén waves, *J. Geophys. Res., 104,* 17,233, 1999.

Ergun, R. E., et al., Fast satellite observations of electric field structures in the auroral zone, *Geophys. Res. Lett., 25,* 2025, 1998.

Génot, V., P. Louarn, and D. Le Quéau, A study of the propagation of Alfvén waves in the auroral density cavities, *J. Geophys. Res., 104,* 22,649, 1999.

Goertz, C., Electron acceleration via kinetic Alfvén waves, in *Etude Comparative des Systèmes Magnétosphériques, La Londe-les-Maures, Septembre 1985, CNES Ed.*, CNES, Toulouse, France, 1986.

Goertz, C., and R. Boswell, Magnetosphere-ionosphere coupling, *J. Geophys. Res., 84,* 7239, 1979.

Gurnett, D. A., R. L. Huff, J. D. Menietti, J. L. Burch, J. D. Winningham, and S. D. Shawhan, Correlated low-frequency electric and magnetic noise along the auroral field lines, *J. Geophys. Res., 89,* 8971, 1984.

Gustafsson, G., M. André, L. Matson, and H. Koskinen,

On waves below the local proton gyrofrequency in auroral acceleration regions, *J. Geophys. Res., 95,* 5889, 1990.

Hasegawa, A., Particle acceleration by MHD surface wave and formation of aurora, *J. Geophys. Res., 81,* 6083, 1976.

Hewett, D., and B. Langdon, Electromagnetic direct implicit plasma simulation, *J. Comput. Physics, 72,* 121, 1987.

Heyvaerts, J., and E. R. Priest, Coronal heating by phase-mixed shear Alfvén waves, *Astron. Astrophys., 117,* 220, 1983.

Hilgers, A., The auroral radiating plasma cavities, *Geophys. Res. Lett., 19,* 237, 1992.

Hilgers, A., B. Holback, G. Holmgren, and R. Boström, Probe measurements of low plasma densities with application to the auroral acceleration regions and auroral kilometric radiation sources, *J. Geophys. Res., 97,* 8631, 1992.

Hockney, R. H., and J. W. Eastwood, in *Computer Simulations Using Particles*, Adam Hilger, New York, 1988.

Kletzing, C. A., Electron acceleration by kinetic Alfvén waves, *J. Geophys. Res., 99,* 11095, 1994.

Knudsen, D. J., Spatial modulation of electron energy and density by nonlinear stationary inertial Alfvén waves, *J. Geophys. Res., 101,* 10761, 1996.

Koskinen, H. J., R. Lundin, and B. Holback, On the plasma environment of solitary waves and weak double layers, *J. Geophys. Res., 95,* 5921, 1990.

Langdon, B., B. Cohen, and A. Friedman, Direct implicit large time-step particle simulations of plasmas, *J. Comput. Phys., 51,* 107, 1983.

Louarn, P., A. Roux, H. de Féraudy, D. Le Quéau, M. André, and L. Matson, Trapped electrons as a free energy source for the auroral kilometric radiation, *J. Geophys. Res., 95,* 5983, 1990.

Louarn, P., J. E. Wahlund, T. Chust, H. de Feraudy, A. Roux, B. Holback, P. O. Dovner, A. I. Eriksson, and G. Holmgren, Observation of kinetic Alfvén waves by the Freja spacecraft, *Geophys. Res. Lett., 21,* 17, 1994.

Lysak, R. L., Electrodynamic coupling of the magnetosphere and ionosphere, *Space Sci. Rev., 52,* 33, 1990.

Lysak, R. L., and C. T. Dum, Dynamics of magnetosphere-ionosphere coupling including turbulent transport, *J. Geophys. Res., 88,* 365, 1983.

Lysak, R. L., and W. Lotko, On the kinetic dispersion relation for shear Alfvén waves, *J. Geophys. Res., 101,* 5085, 1996.

Mälkki, A., A. I. Eriksson, P. O. Dovner, R. Boström, B. Holback, G. Holmgren, and H. Koskinen, A statistical survey of auroral solitary waves and weak double layers, 1, Occurrence and net voltage, *J. Geophys. Res., 98,* 15,521, 1993.

Mangeney, A., C. Salem, C. Lacombe, J.-L. Bougeret, C. Perche, R. Manning, P. J. Kellogg, K. Goetz, S. J. Monson, and J.-M. Bosqued, WIND observations of coherent electrostatic waves in the solar wind, *Ann. Geophys., 17,* 307, 1999.

Malara, F., L. Primavera, and P. Veltri, Formation of small scales via Alfvén wave propagation in compressible nonuniform media, *Astrophys. J., 459,* 347, 1996.

Miura, A., and T. Sato, Numerical simulation of global formation of auroral arcs, *J. Geophys. Res., 85,* 73, 1980.

Mottez, F., G. Chanteur, and A. Roux, Filamentation of plasma in the auroral region by an ion-ion instability: A process for the formation of bidimensional potential structures, *J. Geophys. Res., 97,* 10,801, 1992.

Mottez, F., J. C. Adam, and A. Heron, A new guiding centre PIC scheme for electromagnetic highly magnetized plasma simulation, *Comput. Phys. Commun., 113,* 1, 1998.

Mozer, F. S., and M. Temerin, Solitary waves and double layers as the source of parallel electric fields in the auroral acceleration region, in *High-Latitude Space Plasma Physics*, edited by B. Hultqvist and T. Hagfors, p. 453, Plenum, New York, 1983.

Northrop, T., *The Adiabatic Motion of Charged Particles*, Wiley-Interscience, New York, 1963.

Papadopoulos, K., A review of anomalous resistivity for the ionosphere, *Rev. Geophys., 15,* 113, 1977.

Seyler, C. E., A mathematical model of the structure and evolution of small-scale discrete auroral arcs, *J. Geophys. Res., 95,* 17,199, 1990.

Seyler, C. E., and J. E. Wahlund, Theory of nearly perpendicular electrostatic plasma waves and comparison to Freja satellite observations, *J. Geophys. Res., 101,* 21,795, 1996.

Seyler, C. E., J. E. Wahlund, and B. Holback, Theory and simulation of low-frequency plasma waves and comparison to Freja satellite observations, *J. Geophys. Res., 100,* 21,453, 1995.

Shukla, P. K., L. Stenflo, and R. Bingham, Nonlinear propagation of inertial Alfvén waves in auroral plasmas, *Phys. Plasmas, 6,* 1677, 1999.

Stasiewicz, K., G. Holmgren, and L. Zanetti, Density depletions and current singularities observed by Freja, *J. Geophys. Res., 103,* 4251, 1998.

Strangeway, R. J., et al., Fast observations of VLF waves in the auroral zone: Evidence of very low plasma densities, *Geophys. Res. Lett., 25,* 2065, 1998.

Streltsov, A. V., and W. Lotko, Dispersive field line resonances on auroral field lines, *J. Geophys. Res., 100,* 19,457, 1995.

Streltsov, A. V., and W. Lotko, Small-scale, "electrostatic" auroral structures and Alfvén waves, *J. Geophys. Res., 104,* 4411, 1999.

Temerin, M., C. A. Catell, K. Cerny, W. Lotko, and F. S. Mozer, Observations of double layers and solitary waves in auroral plasma, *Phys. Rev. Lett., 48,* 164, 1982.

Volwerk, M., P. Louarn, T. Chust, A. Roux, H. de Féraudy, and B. Holback, Solitary kinetic Alfvén waves: A study of the Poynting flux, *J. Geophys. Res., 101,* 13,335, 1996.

Wahlund, J. E., P. Louarn, T. Chust, H. de Féraudy, A. Roux, B. Holback, P. O. Dovner, and G. Holmgren, On ion-acoustic turbulence and the nonlinear evolution of kinetic Alfvén waves, *Geophys. Res. Lett., 21,* 1831, 1994.

Weimer, D. R., and D. A. Gurnett, Large-amplitude auroral electric fields measured with DE 1, *J. Geophys. Res., 98,* 13557, 1993.

V. Génot, Astronomy Unit, Queen Mary, University of London, London E1 4NS, England, UK. (v.genot@qmw.ac.uk)

P. Louarn, Centre d'Étude Spatiale des Rayonnements, 9 Av. Colonel Roche, 31400 Toulouse, France. (Philippe.Louarn@cesr.fr)

F. Mottez, Centre d'Étude des Environnements Terrestre et Planétaires, 10-12 Av. de l'Europe, 78140 Vélizy, France. (fabrice.mottez@cetp.ipsl.fr)

(Received September 16, 1999; revised May 8, 2000; accepted June 5, 2000.)